

Operational Space Control for Planar PA^{N-1} Underactuated Manipulators Using Orthogonal Projection and Quadratic Programming

Xiangyu Chu^{a,*}, Yunxi Tang^a, Alessandro M. Giordano^b, Tan Chen^c, and K. W. Samuel Au^a

Abstract—In this paper, we propose an operational space control formulation for a planar N -link underactuated manipulator (PA^{N-1})¹ with a passive first joint subject to actuator constraints ($N \geq 3$), covering both stabilization and tracking tasks. Such underactuated manipulators have an inherent first-order nonholonomic constraint, allowing us to project their dynamics to a space consistent with the nonholonomic constraint. Based on the constrained dynamics, we can design operational space controllers with respect to tasks assuming that all joints of the manipulator are active. Due to underactuation, we design a Quadratic Programming (QP) based controller to minimize the error between the desired torque commands and available motor torques in the null space of the constraint, as well as involve the constraint of motor outputs. The proposed control framework was demonstrated by stabilization and tracking tasks in simulations with both planar PA^2 and PA^3 manipulators. Furthermore, we verified the controller experimentally using a planar PA^2 robot.

I. INTRODUCTION

Underactuated manipulators, which have fewer number of control inputs than degrees of freedom, have attracted researchers in both control and robotics communities. It is known that underactuated manipulators² can be divided into two main types: Vertical Underactuated Manipulators (VUM) and Horizontal Underactuated Manipulators (HUM). Due to the presence of gravity, the control of VUMs mostly focuses on the stabilization of the vertical unstable equilibrium position at which their linearized model is locally controllable [1]. However, the control of HUMs like stabilizing the end-effector is particularly challenging since the linearized model at any equilibrium position is not controllable because of the absence of gravity [2]. A general nonlinear control method is not yet available, thus the control design depends on what constraint the system owns according to integrability conditions [3], e.g., a second-order nonholonomic constraint [4], a first-order nonholonomic constraint [8], or a holonomic constraint [5]. Although there is a large amount of existing work devoted to controlling specific or a class of HUMs,

the development of systematic and efficient controllers remains open. Especially for the planar horizontal N -link underactuated manipulator with a passive first joint (denoted as planar PA^{N-1} manipulator, $N \geq 3$) which has a first-order nonholonomic constraint, to the best of our knowledge only a few limited solutions are available in the literature. Therefore, in this paper, we restrict our attention to the operational space control of planar PA^{N-1} manipulators.

In the control community, researchers started from planar PA^2 manipulators that were in low dimension. Their operational space control design was significantly different from common practice in fully-actuated or redundant manipulators, e.g., using operational space frameworks in [14]. Firstly, the control was not accomplished at the task space level, but at the joint space level; optimization or searching methods were used to determine the desired joint configuration with respect to the desired end-effector position, such as genetic algorithm [8], differential evolution algorithm [9] and particle swarm optimization [10], [11]. Secondly, several control strategies were designed to force the joints to achieve the desired ones, such as Lyapunov function methods [8], [11] and model reduction to planar Acrobot [10]. However, the resulting controllers in [10], [11] were two-stage control with switching. And [9], [10] required the explicit relation between the passive joint and active joints for their planning process, which may hinder their methods from being scaled up to a general case due to extensive derivation efforts.

Subsequently, researchers in the control community studied general planar PA^{N-1} manipulators. Prohibited by the increasing computation cost, the idea of planning for each joint was not directly extended. The model reduction became more appealing in high-dimensional planar PA^{N-1} manipulators, e.g., only keeping two joints active and maintaining other $N - 3$ active joints at zero angle. Thus, the original manipulator can be reduced to a virtual planar three-link one [12], [13] and then the method developed in planar PA^2 manipulators can be used. Although their solutions were able to stabilize the end-effector to a desired position, they suffered from complex design and realization. Model reduction allowed one to reuse previous solutions, but it limited the capability of the original manipulator, i.e., the $N - 3$ active joints ($N > 3$) that were keeping zero should have provided degrees of freedom for secondary tasks. Moreover, most mentioned work involved optimization or searching techniques offline and thus they may not be able to reject external disturbance and uncertainty in real time. Besides, no experiment has been provided in the mentioned

This work is supported by CUHK Chow Yuk Ho Technology Centre of Innovative Medicine, MRC, InnoHK, RGC GRF Ref No. 14209719, 14209118, RGC T42-409/18-R, and Natural Science Foundation of China, U1613202.

^aDepartment of Mechanical and Automation Engineering, The Chinese University of Hong Kong, Hong Kong, China. ^bInstitute of Robotics and Mechatronics, German Aerospace Center (DLR), 82234 Weßling, Germany. ^cDepartment of Aerospace and Mechanical Engineering, University of Notre Dame, IN 46556, USA. *Corresponding author: xychu@mae.cuhk.edu.hk.

¹Denoting planar horizontal N -link underactuated manipulator with a passive first joint as planar PA^{N-1} manipulator, where “P” means a passive joint and “A” means an active joint. The first letter denotes the first joint.

²Assuming manipulators only have revolute joints.

work. Overall, a simple, real-time, and efficient feedback controller with more control capability for the operational space control of planar PA^{N-1} underactuated manipulators is desired.

In the robotics community, operational space control has been extensively studied since it provides us with standard solutions to obtain desired behavior of tasks. Except for well-built control frameworks for fully-actuated and redundant systems, researchers show an increasing interest in designing task-oriented controllers for underactuated systems. Based on a unified formulation on the operational space framework [14], some researchers extended it to underactuated systems, such as free-floating humanoid robots [15], quadrupedal robots [16], orbital robots [17], aerial robots [18], and planar underactuated manipulators with a passive third joint [19]. There were two main solutions to the extension: 1) Quadratic Programming (QP)-based prioritized control (or iterative null-space projection) [16], [20]–[22]; 2) projection-based control [15], [19], [23], [24], which can deal with constraints and underactuation in different way. For example, [21] proposed a constrained prioritized multi-objective QP-based control formulation. Different from previous work, the defined tasks were not desired motions or desired constraint forces, but desired feedback control laws that were designed based on the model of the robot and environment. Due to underactuation, exact realization of desired control laws was infeasible and QP was used for minimizing the error between the desired and actual control. [23] and [24] proposed different projection operators, but both of them could eliminate Lagrange multipliers (e.g., constraint forces) and obtain a constrained inverse dynamics equation. However, they may not be able to involve actuation limitations.

In this paper, we propose an operational space control formulation for planar PA^{N-1} manipulators using orthogonal projection and QP. *The main strategy is to leverage on the projection operator (e.g., linear projection) in order to obtain constrained dynamics, and on the optimization method (e.g., QP) in order to maximize the ability of implementing the desired control law considering underactuation.* As mentioned before, planar PA^{N-1} manipulators have an inherent first-order nonholonomic constraint, allowing us to create a projection matrix that can project a space into the null space of the constraint mapping. With the projection operator, we can obtain a projected dynamics, i.e., the original dynamics is projected into a space consistent with the nonholonomic constraint or the null space of the constraint. With geometry properties in [23], we can obtain a constrained dynamics that incorporates the inherent constraint and owns a passivity property. Note that our projection matrix stems from a first-order nonholonomic constraint, while existing work mostly generates a projection matrix based on task constraints [22] or physical contact constraints [24].

With the resulting constrained dynamics, we can design task-oriented operational space controllers according to the task we want to implement assuming that all joints are active. However, underactuation in the manipulator limits the exact implementation of the desired control commands

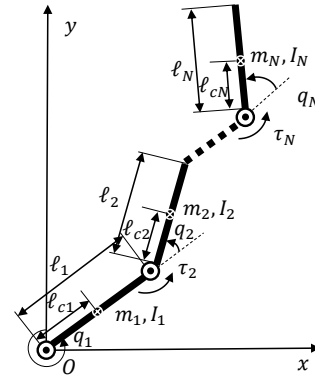


Fig. 1: Planar N -link underactuated manipulators with a passive first joint in the absence of gravity. The first joint is passive and connected to a base, while the rest of joints are active.

generated by those task-oriented controllers. Inspired by the use of QP in [22], we design a QP-based controller based on the constrained dynamics to maximize the capability of implementing the control commands.

Overall, the key contributions of this paper are:

- 1) Proposing an operational space control formulation for planar PA^{N-1} manipulators that can provide simple, real-time, and efficient control solutions to both stabilization and tracking tasks, as well as utilize redundancy if any;
- 2) Utilizing a first-order nonholonomic constraint in planar PA^{N-1} manipulators to obtain a constrained dynamics and formulating a general QP problem that can integrate different task-oriented controllers and input limitations;
- 3) Demonstrating the proposed formulation in experiments based on a newly-designed planar PA^2 platform with negligible gravity effects.

II. MODELLING

A. Inherent Constraint

Considering a planar N -link underactuated manipulator with a passive first joint, its Lagrange equation describing the motion can be written as

$$\frac{d}{dt} \left(\frac{\partial L}{\partial \dot{q}_n} \right) - \frac{\partial L}{\partial q_n} = \tau_n, \quad n = 1, 2, \dots, N, \quad (1)$$

where L denotes Lagrangian, q_n denotes the generalized coordinate, and τ_n denotes the generalized force. Note that here Lagrangian is only related to the total system kinetic energy since the system is in the absence of gravity. The first joint is passive and the rest of joints are active. A matrix form of the dynamics is given by

$$\mathbf{M}(\mathbf{q})\ddot{\mathbf{q}} + \mathbf{C}(\mathbf{q}, \dot{\mathbf{q}})\dot{\mathbf{q}} = \mathbf{B}\mathbf{u}, \quad (2)$$

where $\mathbf{q} = [q_1, q_2, \dots, q_N]^T$ denotes the generalized state vector, $\mathbf{M}(\mathbf{q}) \in \mathbb{R}^{N \times N}$ denotes the symmetric and positive-definite inertia matrix, and $\mathbf{C}(\mathbf{q}, \dot{\mathbf{q}}) \in \mathbb{R}^N$ denotes Coriolis and centrifugal forces. $\mathbf{B} = [\mathbf{0}_{(N-1) \times 1}^T \quad \mathbf{I}_{(N-1) \times (N-1)}]^T$ is the actuator matrix corresponding to $N-1$ active joints and $\mathbf{u} = [\tau_2, \tau_3, \dots, \tau_N]^T$ is the actuator torque vector.

To show the inherent first-order nonholonomic constraint in the system, we recall (1) with $n = 1$, i.e.,

$$\frac{d}{dt} \left(\frac{\partial L}{\partial \dot{q}_1} \right) - \frac{\partial L}{\partial q_1} = 0, \quad (3)$$

where $L = \frac{1}{2}\dot{\mathbf{q}}^T \mathbf{M}(\mathbf{q})\dot{\mathbf{q}}$. According to [3], the planar underactuated manipulator with a passive first joints owns the property of partial integrability since the inertia matrix $\mathbf{M}(\mathbf{q})$ does not depend on q_1 and there is no gravity, thus $\frac{\partial L}{\partial q_1} = 0$. Further, the first term of (3) is computed as $\frac{\partial L}{\partial \dot{q}_1} = \frac{\partial}{\partial \dot{q}_1}(\frac{1}{2}\dot{\mathbf{q}}^T \mathbf{M}(\mathbf{q})\dot{\mathbf{q}}) = \sum_{n=1}^N M_{1n}(\mathbf{q})\dot{q}_n$. Therefore, integrating (3) yields the inherent constraint of the manipulator,

$$\sum_{n=1}^N M_{1n}(\mathbf{q})\dot{q}_n = \sum_{n=1}^N M_{1n}(\mathbf{q}_0)\dot{q}_{n0}, \quad (4)$$

where \mathbf{q}_0 is the initial joint configuration and $\dot{\mathbf{q}}_{n0}$ is the initial angular velocity of the n -th joint [6]. A specific expression of (4) for $N = 3$ can be found in [7]. Any admissible $\dot{\mathbf{q}}$ should satisfy this constraint.

Therefore, unlike other types of planar underactuated manipulators with the second-order nonholonomic constraint, the planar PA^{N-1} manipulator has an inherent first-order constraint, as given by (4). The quantity (4) is referred to as angular momentum conjugate to q_1 .

B. Constrained Dynamics with Orthogonal Projection

Previous work focused on constrained underactuated systems, like underactuated manipulators with tip contact constraints [19] and humanoid robots with foot contact constraints [24]. An effective way is to eliminate their constraint forces by projection and thus the constrained dynamics can be obtained. Motivated by this idea, we approach the constrained dynamics of the planar PA^{N-1} manipulator by orthogonal projection related to the inherent constraint (4) with an assumption.

Assumption 1: The manipulator starts from a static state. The constraint (4) can be written in the Pfaffian form

$$\mathbf{A}(\mathbf{q})\dot{\mathbf{q}} = 0. \quad (5)$$

$\mathbf{A}(\mathbf{q}) \in \mathbb{R}^{1 \times N} = [M_{11}, M_{12}, \dots, M_{1N}]^T$ is the *constraint mapping* and the joint velocity has to be in the null space of the constraint. $\mathbf{P} = \mathbf{I}_{N \times N} - \mathbf{A}^+ \mathbf{A}$ is called as null-space projection matrix, where $(\bullet)^+$ represents the Moore–Penrose pseudoinverse such that $\mathbf{A}^+ = \mathbf{A}^T (\mathbf{A} \mathbf{A}^T)^{-1}$ and the function dependency is omitted for simplicity. There exists a relation $\mathbf{P}\dot{\mathbf{q}}_{null} = \dot{\mathbf{q}}$, if (5) is satisfied, where $\dot{\mathbf{q}}_{null}$ denotes the the velocity vector in the null space of \mathbf{A} . In this paper, the discussed system inherently satisfies the constraint (5) because the system starts from static states and has the property of angular momentum conservation. Thus, we have³

$$\mathbf{P}\dot{\mathbf{q}} = \dot{\mathbf{q}}. \quad (6)$$

Pre-multiplying both sides of (2) with \mathbf{P} yields

$$\mathbf{P}\mathbf{M}\ddot{\mathbf{q}} + \mathbf{P}\mathbf{C}\dot{\mathbf{q}} = \mathbf{P}\mathbf{B}\mathbf{u}, \quad (7)$$

where (7) can be considered as *projected dynamics* in the null space of the constraint. However, $\mathbf{P}\mathbf{M}$ is not invertible since \mathbf{P} is generally rank deficient ($\text{rank}(\mathbf{P}) = N - 1$).

To make the inertia matrix invertible, different ideas have been proposed. [26] provided one treatment that can keep fundamental properties in normal Lagrange formulations. Specifically, substituting (6) and its time derivative into (7)

yields

$$\mathbf{P}\mathbf{M}\mathbf{P}\ddot{\mathbf{q}} + (\mathbf{P}\mathbf{C} + \mathbf{P}\dot{\mathbf{M}}\mathbf{P})\dot{\mathbf{q}} = \mathbf{P}\mathbf{B}\mathbf{u}. \quad (8)$$

Taking time derivative of $(\mathbf{I} - \mathbf{P})\dot{\mathbf{q}} = \mathbf{0}$ gives

$$(\mathbf{I} - \mathbf{P})\ddot{\mathbf{q}} + \mathbf{A}^+ \dot{\mathbf{A}}\dot{\mathbf{q}} = \mathbf{0}. \quad (9)$$

The *constrained dynamics* is obtained by adding (8) and (9)

$$\bar{\mathbf{M}}\ddot{\mathbf{q}} + \bar{\mathbf{C}}\dot{\mathbf{q}} = \mathbf{P}\mathbf{B}\mathbf{u}, \quad (10)$$

where $\bar{\mathbf{M}} := \mathbf{P}\mathbf{M}\mathbf{P} + \mathbf{I} - \mathbf{P}$ and $\bar{\mathbf{C}} := \mathbf{P}\mathbf{C}\mathbf{P} + \mathbf{P}\dot{\mathbf{M}}\mathbf{P} + \mathbf{A}^+ \dot{\mathbf{A}}\mathbf{P}$. $\bar{\mathbf{M}}$ is called as *constraint inertia matrix*, which is symmetric and positive-definite. Note that $\bar{\mathbf{M}} - 2\bar{\mathbf{C}}$ is a skew-symmetric matrix. These two fundamental properties have been proved in [26].

What we want to emphasize is that the projection used is based on a “virtual” first-order nonholonomic constraint inside the manipulator, different from those systems with physical constraints. Interestingly, we can still formulate the original dynamics of the planar PA^{N-1} manipulator as the form of the constrained dynamics. Such a formulation paves the way to the design of operational space controllers.

III. OPERATIONAL SPACE CONTROL FORMULATION

In this section, we will present the proposed operational control formulation with two parts: task-oriented control and QP-based control.

A. Task-Oriented Controllers

Given a task variable $\mathbf{x}(\mathbf{q}) \in \mathbb{R}^m$ ($1 \leq m \leq N - 1$), the *task Jacobian* $\mathbf{J} \in \mathbb{R}^{m \times N}$ is defined by the relation

$$\dot{\mathbf{x}} = \mathbf{J}\dot{\mathbf{q}}, \quad (11)$$

where $\mathbf{J} = \frac{\partial \mathbf{x}}{\partial \mathbf{q}} \mathbf{P}$ and $\mathbf{P}\dot{\mathbf{q}} = \dot{\mathbf{q}}$ are used. Note that the inherent constraint has been integrated into the task Jacobian for consistency. Naturally, important relations occur

$$\mathbf{J}\mathbf{P} = \mathbf{J} \text{ and } \mathbf{J}^T = \mathbf{P}\mathbf{J}^T. \quad (12)$$

Taking the time derivative of (11) yields

$$\ddot{\mathbf{x}} = \mathbf{J}\ddot{\mathbf{q}} + \dot{\mathbf{J}}\dot{\mathbf{q}}, \quad (13)$$

where $\dot{\mathbf{J}} = \frac{d}{dt}(\frac{\partial \mathbf{x}}{\partial \mathbf{q}}) \mathbf{P} + \frac{\partial \mathbf{x}}{\partial \mathbf{q}} \dot{\mathbf{P}}$ and $\dot{\mathbf{P}} = -\mathbf{A}^+ \dot{\mathbf{A}} \mathbf{P} - \mathbf{P}\dot{\mathbf{A}}^T \mathbf{A}^{+T}$ according to [28].

To achieve the operational space control, we first assume all joints of the manipulator are active by replacing⁴ $\mathbf{B}\mathbf{u}$ with the generalized force vector $\boldsymbol{\tau}_{osc} \in \mathbb{R}^N$, thus the constrained dynamics is updated to

$$\bar{\mathbf{M}}\ddot{\mathbf{q}} + \bar{\mathbf{C}}\dot{\mathbf{q}} = \mathbf{P}\boldsymbol{\tau}_{osc}. \quad (14)$$

Based on (14), we can design a desired control law $\boldsymbol{\tau}_{osc}$ to achieve the desired task assuming \mathbf{J} is full rank⁵.

1) *PD Controller:* The goal is to stabilize the planar PA^{N-1} manipulator from an initial task variable \mathbf{x}_0 to a desired task variable \mathbf{x}_d . Here we choose a PD controller in [25] (Chapter 8.6), i.e.,

$$\boldsymbol{\tau}_{osc} = \mathbf{J}^T \mathbf{K}_p \mathbf{e} - \mathbf{J}^T \mathbf{K}_d \mathbf{J}\dot{\mathbf{q}}, \quad (15)$$

where $\mathbf{K}_p > 0$, $\mathbf{K}_d > 0$, and $\mathbf{e} = \mathbf{x}_d - \mathbf{x}$. If the task variable involves spatial rotation, the error can be calculated

⁴This assumption has been used in [22]. Eq. (14) implies that only the generalized force in the null space of the constraint contributes to the motion of the manipulator.

⁵This could be ensured by a suitable trajectory planning [29].

³With a slight abuse of notation, we replace $\dot{\mathbf{q}}_{null}$ with $\dot{\mathbf{q}}$.

by using angle and axis or quaternions [25]. The second term is used to enhance system damping. Substituting (15) into (14) generates the closed-loop control system

$$\bar{M}\ddot{q} + \bar{C}\dot{q} = PJ^T K_p e - PJ^T K_d J\dot{q}. \quad (16)$$

Choosing a Lyapunov function

$$V = \frac{1}{2}\dot{q}^T \bar{M}\dot{q} + \frac{1}{2}e^T K_p e, \quad (17)$$

we substitute (16) to its time derivative

$$\begin{aligned} \dot{V} &= \dot{q}^T \bar{M}\ddot{q} + \frac{1}{2}\dot{q}^T \dot{\bar{M}}\dot{q} + e^T K_p \dot{e} \\ &= \frac{1}{2}\dot{q}^T (\dot{\bar{M}} - 2\bar{C})\dot{q} + \dot{q}^T J^T K_p e - \dot{q}^T J^T K_d J\dot{q} \\ &\quad - \dot{q}^T J^T K_p e = -\dot{q}^T J^T K_d J\dot{q} \leq 0, \end{aligned} \quad (18)$$

where (12) is used. Equation (18) shows that V decreases for any $\dot{q} \neq \mathbf{0}$ and the system will reach an equilibrium posture. Substituting $\dot{q} = \ddot{q} = \mathbf{0}$ into (16) can determine the equilibrium posture as

$$PJ^T K_p e = J^T K_p e = \mathbf{0}.$$

Only $e = \mathbf{0}$ satisfies this equilibrium posture as $J^T K_p$ is full rank. In other words, the controller (15) can stabilize the manipulator to a desired task x_d .

2) *Inverse Dynamics Controller*: The goal is to design a controller such that the end-effector of the manipulator can track a desired trajectory $x_d(t)$. To this end, we pre-multiply both sides of (14) by $J\bar{M}^{-1}$,

$$J\ddot{q} + J\bar{M}^{-1}\bar{C}\dot{q} = J\bar{M}^{-1}P\tau_{osc}, \quad (19)$$

and then we substitute (13) and $\tau_{osc} = J^T F$,

$$\Lambda\ddot{x} + \Lambda(J\bar{M}^{-1}\bar{C} - \dot{J})\dot{q} = F,$$

where $\Lambda = (J\bar{M}^{-1}PJ^T)^{-1} = (J\bar{M}^{-1}J^T)^{-1}$ and F is the force at the end-effector. Inspired by [14], the controller is designed as

$$\tau_{osc} = J^T F + (I - J^T J^{T\#})\tau_0. \quad (20)$$

where

$$\begin{aligned} F &= \Lambda(\ddot{x}_d + K_d \dot{e} + K_p e) + \Lambda(J\bar{M}^{-1}\bar{C} - \dot{J})\dot{q}, \\ J^{T\#} &= (J\bar{M}^{-1}PJ^T)^{-1}J\bar{M}^{-1}P, \end{aligned}$$

$e(t) = x_d(t) - x(t)$, and an arbitrary joint force vector τ_0 does not affect the end-effector. The term $(I - J^T J^{T\#})\tau_0$ is the joint force corresponding to a null space operational force vector if there is redundancy. Note that τ_0 is trivial if $m = N - 1$. In this case, substituting (20) into (19) yields the tracking error dynamics

$$\ddot{e} + K_d \dot{e} + K_p e = \mathbf{0}, \quad (21)$$

which shows that the control can achieve asymptotic operational space tracking. Moreover, this controller also works for stabilization tasks.

The design of τ_0 can be driven by many purposes, such as limiting the joint range and avoiding singularities. Specifically, based on (14), we have

$$\tau_0 = \bar{M}\ddot{q}_0 + \bar{C}\dot{q}_0, \quad \ddot{q}_0 = \frac{d}{dt}\dot{q}_0, \quad (22)$$

where \dot{q}_0 is typically chosen as $\dot{q}_0 = -k_0(\frac{\partial H(q)}{\partial q})^T$, $k_0 > 0$, and $H(q) \geq 0$ is a secondary objective function of joint variables. To demonstrate the effectiveness of the secondary

task, we present an example, i.e., limiting joint ranges,

$$H(q) = \frac{1}{2n} \sum_{i=1}^n \left(\frac{q_i - \bar{q}_i}{q_{M,i} - q_{m,i}} \right)^2, \quad (23)$$

where $\bar{q}_i = \frac{q_{M,i} + q_{m,i}}{2}$ and $q_i \in [q_{m,i}, q_{M,i}]$ [25]. This renders that we can expect a desired configuration at the end of the main task, especially for a large N .

B. QP-based Controller

With a desired control law τ_{osc} , the goal is to determine the control input u in the original dynamics that can exactly reproduce τ_{osc} . Mathematically, if we relax the equality relation to an optimization problem, such a goal can be illustrated as

$$u^* = \arg \min_{u_{min} \leq u \leq u_{max}} \|Bu - \tau_{osc}\|^2, \quad (24)$$

where u_{min} and u_{max} are the lower bound and upper bound of actuator torques. Due to underactuation, the manipulator cannot exactly implement the desired torque commands even if we remove the actuation constraint. Similar issues have been reported in [22] and they decomposed the error norm into task-space and self-motion space norms. It was because they enforced the system to comply with a user-defined task constraint $\Phi(q, t) = \mathbf{0}$. Thus, the task-space norm was corresponding to the range space of Γ while the self-motion space norm was corresponding to the null space of Γ , where $\Gamma = \partial\Phi/\partial q$. Inspired by [22], we can decompose (24) as

$$\|Bu - \tau_{osc}\|^2 = \|Bu - \tau_{osc}\|_P^2 + \|Bu - \tau_{osc}\|_{I-P}^2. \quad (25)$$

In our case, the manipulator is inherently enforced by a first-order nonholonomic constraint $A(q)\dot{q} = 0$, which implies that all admissible motions should be in the null space of A (or, equivalently, in the range space of P). Since the design of τ_{osc} is based on the constrained dynamics, the resulting τ_{osc} is in the null space of the constraint. $\|Bu - \tau_{osc}\|_P^2$ can be effective to minimize the total error $\|Bu - \tau_{osc}\|^2$, however, $\|Bu - \tau_{osc}\|_{I-P}^2$ would increase the total error for any u^* . To minimize the error in (24) effectively, a QP-based formulation with additionally introducing a damping term (e.g., $u^T u$) is designed as

$$\min_{u_{min} \leq u \leq u_{max}} \frac{1}{2}\|u\|^2 + r\|Bu - \tau_{osc}\|_P^2 \quad (26)$$

where $r > 0$. Note that τ_{osc} is calculated based on the constrained dynamics encoded by the nonholonomic constraint, instead of the original dynamics. Equation (26) specifically minimizes the total error in the range space of P , which emphasizes the importance of orthogonal projection.

IV. SIMULATIONS

In this section, planar PA² and PA³ manipulators are used to demonstrate the effectiveness of the proposed operational space control formulation. For comparison, the model parameters of the manipulators, the initial configurations, and the desired tasks are chosen from [8] (PA²) and [12] (PA³). For all simulations, the original dynamics (2) was applied.

A. Planar PA² Manipulator

1) *Stabilization Task*: The initial configuration was set as $q_0 = [1.6, 0.9, 0.5]^T$ and the initial angular velocity was

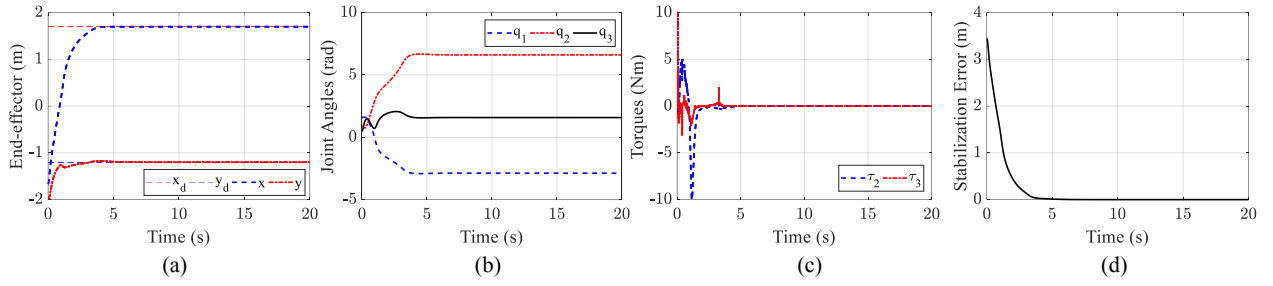


Fig. 2: Simulation results of the planar PA^2 manipulator on the stabilization task using the control (15) and (26). (a) Position of the end-effector; (b) Joint angles of the manipulator; (c) Torque profiles of the active joints; (d) Stabilization error of the end-effector.

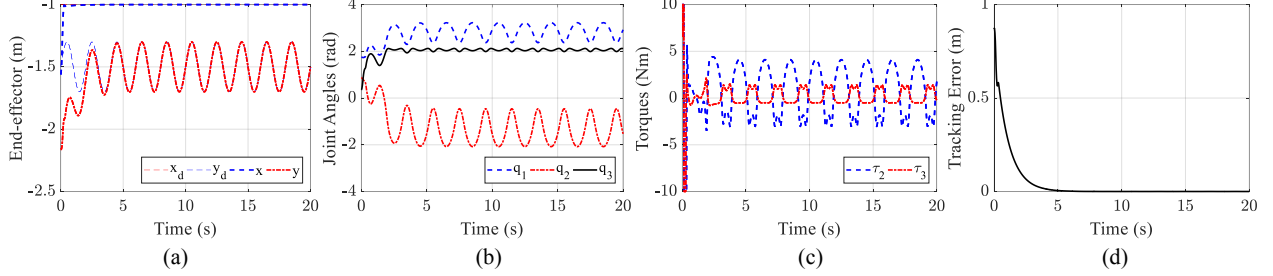


Fig. 3: Simulation results of the planar PA^2 manipulator on the tracking task using the control (20) and (26). (a) Position of the end-effector; (b) Joint angles of the manipulator; (c) Torque profiles of the active joints; (d) Tracking error of the end-effector.

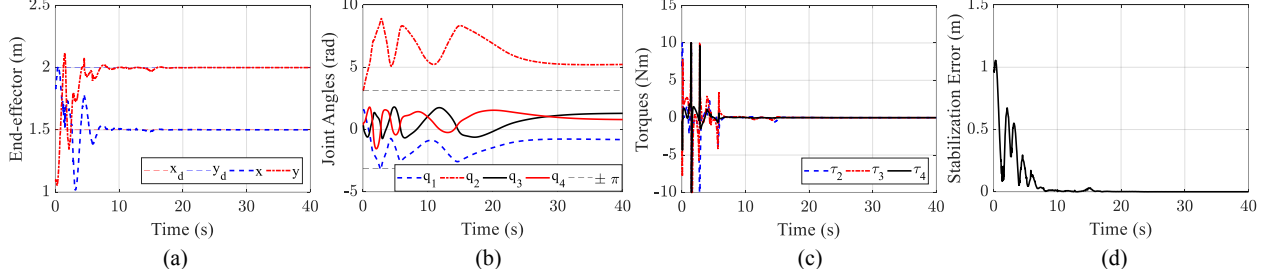


Fig. 4: Simulation results of the planar PA^3 manipulator on the stabilization task using the control (20) and (26). (a) Position of the end-effector; (b) Joint angles of the manipulator; (c) Torque profiles of the active joints; (d) Stabilization error of the end-effector.

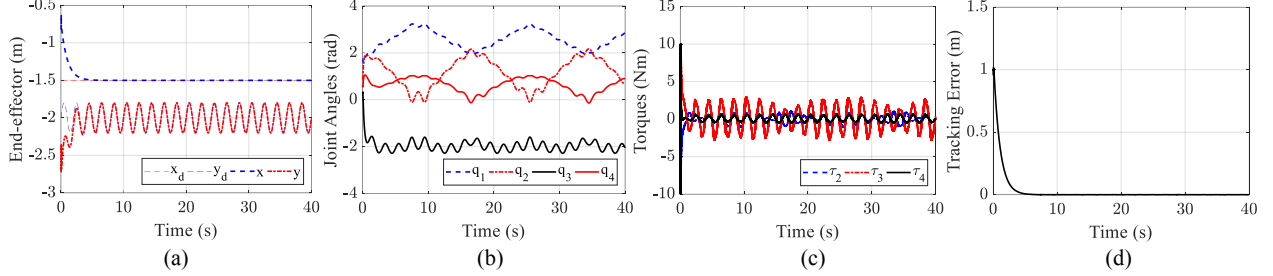


Fig. 5: Simulation results of the planar PA^3 manipulator on the tracking task using the control (20) and (26). (a) Position of the end-effector; (b) Joint angles of the manipulator; (c) Torque profiles of the active joints; (d) Tracking error of the end-effector.

zero. The task was to stabilize the position of the end-effector (x, y) to $(x_d, y_d) = (1.7, -1.2)$ m. In simulations, we first used the controller (15) to calculate the desired operational space control command τ_{osc} , where $\mathbf{K}_p = 50\mathbf{I}_{2 \times 2}$ and $\mathbf{K}_d = 50\mathbf{I}_{2 \times 2}$. Then at each step, the calculated τ_{osc} was fed to the QP computation (26) with $r = 1$. As shown in Fig. 2 (a), the desired task was achieved and the end-effector was stabilized to the desired position with a steady-state error norm less than 2.6×10^{-5} m. As expected, the motor torque evolved within the limitation ($[-10, 10]$ Nm). We noticed that the same task had been manipulated based on the same manipulator in [8], however, they used an off-line searching method to determine the desired joint configuration

and control gains given initial configurations and desired task variables. Although [8] achieved the task, our method showed significant advantages on control design (no searching was included) and realization (real time implementation was feasible).

2) *Tracking Task*: The initial configuration was arbitrarily set as $\mathbf{q}_0 = [100^\circ, 50^\circ, 20^\circ]^T$ and the initial angular velocity was zero. The end-effector was expected to track a trajectory $[-1, 0.2 \sin(\pi t) - 1.5]^T$ m. The controller (20) was used with $\mathbf{K}_p = 100\mathbf{I}_{2 \times 2}$, $\mathbf{K}_d = 100\mathbf{I}_{2 \times 2}$, and $\tau_0 = \mathbf{0}$. The resulting torque command was used in (26) with $r = 50$. The tracking task with limited torque output was achieved with an error bound of 2.69×10^{-4} m, as shown in Fig. 3.

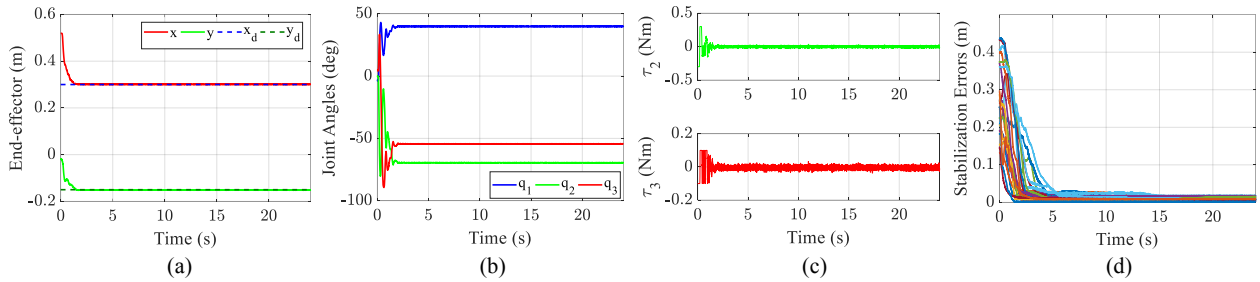


Fig. 6: Experimental results of the planar PA^2 manipulator on the stabilization task using the control (15) and (26). (a)-(c): Evolution of one trial; (d) Stabilization errors of 20 trials ($\|\mathbf{x}_d - \mathbf{x}\|_2$).

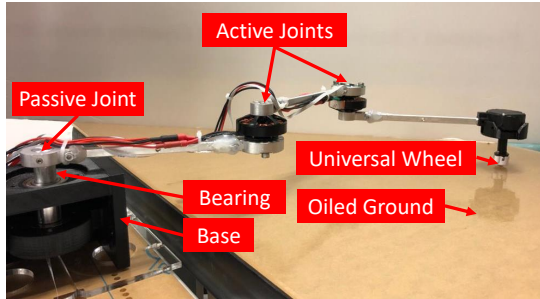


Fig. 7: Planar PA^2 underactuated robot.

B. Planar PA^3 Manipulator

1) *Stabilization Task*: The initial configuration was set as $\mathbf{q}_0 = [\frac{\pi}{2}, \pi, \frac{\pi}{8}, \frac{\pi}{8}]^T$ and the initial angular velocity was zero. Here we used the controller (20) to stabilize the end-effector position (x, y) to $(x_d, y_d) = (1.5, 2)$ m, where $\mathbf{K}_p = 10\mathbf{I}_{2 \times 2}$, $\mathbf{K}_d = 3\mathbf{I}_{2 \times 2}$. The secondary task will be included in this manipulator since the planar PA^3 manipulator is redundant with respect to the task variable. Specifically, (22) and (23) were used with $k_0 = 10$, $q_{m,1} = q_{m,3} = q_{m,4} = -\pi$, and $q_{M,1} = q_{M,3} = q_{M,4} = \pi$. No limitation was enforced to the second joint. The resulting torque command was used in (26) with $r = 1.5$. Again, we repeated the same simulation as [12] did by using our controllers. Fig. 4 shows the manipulator can be stabilized to the desired position with constrained torques and expected joint ranges (steady-state error norm: $< 4.64 \times 10^{-4}$ m). Note that trajectories without oscillations can be achieved if no secondary task is involved. However, [12] reduced a four-link manipulator to a three-link one and applied a discontinuous two-stage control with a searching algorithm, which was more complex and lack of using redundancy.

2) *Tracking Task*: The initial configuration was arbitrarily set as $\mathbf{q}_0 = [100^\circ, 50^\circ, 20^\circ, 30^\circ]^T$ and the initial angular velocity was zero. The end-effector was expected to track a trajectory $[-1.5, 0.2 \sin(\pi t) - 2]^T$ m. The controller (20) was used with $\mathbf{K}_p = 200\mathbf{I}_{2 \times 2}$, $\mathbf{K}_d = 200\mathbf{I}_{2 \times 2}$, and $\boldsymbol{\tau}_0 = \mathbf{0}$. The resulting torque command was used in (26) with $r = 10$. Fig. 5 shows that the tracking task with limited torques was achieved (error bound: $< 5.84 \times 10^{-4}$ m).

V. INITIAL EXPERIMENTS

A planar PA^2 robot was designed, as shown in Fig. 7. The first joint was connected to a revolute bearing which was attached to a base, while the rest of two joints were

actuated by brushless DC motors (T-motor: MN4006). To alleviate the deformation of linkages and reduce the effect of gravity, a support with a universal wheel was designed, although this support would introduce unavoidable frictions between the wheel and oiled ground. The joint angles were measured by using AS5047D magnetic encoders and VESC was used for motor control. A wireless network was used to transfer the data between a remote computer and a single board computer (Raspberry Pi).

Here we will show the results of stabilization tasks and the tracking validation is subject of future work. Figs. 6 (a-c) show one trial evolution, where $\mathbf{K}_p = \text{diag}([45, 60])$, $\mathbf{K}_d = 30\mathbf{I}_{2 \times 2}$ were used. The torque limitations for the second and third joint were 0.3Nm and 0.1Nm, respectively. The end-effector position was estimated by forward kinematics. The robot converged but with a steady-state error (~ 0.003 m), which may be caused by the friction between the support and ground since it became dominant when the end-effector was close to the desired position. Fig. 6 (d) shows the stabilization errors of 20 trials (error bound: < 0.018 m) with various initial positions and desired positions, further demonstrating the effectiveness of the proposed control formulation.

VI. DISCUSSION AND CONCLUSION

In the simulations, stabilization or tracking errors could be observed, but they were in a small scale. The errors can be further reduced if we tune down the tolerance in the numerical solver. The method assumes that the total angular momentum is zero, but the experiments show that the proposed controller can still achieve acceptable results in practice even in the presence of the small non-zero angular momentum injected by the friction with the ground and by the power cable.

In this paper, we presented an operational space control formulation for a class of underactuated manipulators, planar PA^{N-1} underactuated manipulators. By using the techniques of orthogonal projection and QP, we provided a simple control solution, which showed advantages over those solutions in previous work in terms of design efforts, real-time realization, and exploiting available redundancy. In the future, we will devote to extending the proposed formulation to the case of non-zero angular momentum. The experimental setup will be improved to remove the friction caused by the support. Moreover, we desire to generalize the proposed formulation to a large class systems with a conserved quantity like free-floating space robots [17], [30].

REFERENCES

- [1] Alexander Shkolnik and Russ Tedrake. "High-dimensional underactuated motion planning via task space control," *Proceeding of IEEE/RSJ International Conference on Intelligent Robots and Systems*, pp. 3762-3768, 2008.
- [2] Tan Chen and Bill Goodwine. "Controllability and Accessibility Results for an N-Link Horizontal Planar Pendubot," *Proceeding of European Control Conference*, pp. 2596-2602, 2019.
- [3] Giuseppe Oriolo and Yoshihiko Nakamura. "Control of Mechanical Systems with Second-Order Nonholonomic Constraints: Underactuated Manipulators," *Proceeding of IEEE Conference on Decision and Control*, pp. 2398-2403, 1991.
- [4] Jundong Wu, Wenjun Ye, Yawu Wang, and Chun-Yi Su. "A General Position Control Method for Planar Underactuated Manipulators With Second-Order Nonholonomic Constraints," *IEEE Transactions on Cybernetics*, early access, pp. 1-10, 2019.
- [5] Guang-Ping He, Zhi-Lu Wang, Jie Zhang, and Zhi-Yong Geng. "Characteristics analysis and stabilization of a planar 2R underactuated manipulator," *Robotica*, Vol. 34, pp. 584-600, 2016.
- [6] Tan Chen and Bill Goodwine. "Controllability and accessibility results for N-link horizontal planar manipulators with one unactuated joint," *Automatica*, Vol. 125, 109480, 2021.
- [7] Xiangyu Chu, C. H. David Lo, and K. W. Samuel Au. "A Novel Strategy for Stabilization Control of a Planar Three-Link Underactuated Manipulator with a Passive First Joint," *Proceeding of American Control Conference*, pp. 5262-5268, 2020.
- [8] Xuzhi Lai, Pan Zhang, Yawu Wang, Luefeng Chen, and Min Wu. "Continuous State Feedback Control Based on Intelligent Optimization for First-Order Nonholonomic Systems," *IEEE Transactions on Systems, Man, and cybernetics: Systems*, Vol. 50,, No. 7, pp. 2534-2540, 2020.
- [9] Pan Zhang, Xuzhi Lai, Yawu Wang, and Min Wu. "Motion planning and adaptive neural sliding mode tracking control for positioning of uncertain planar underactuated manipulator," *Neurocomputing*, Vol. 334, pp. 197-205, 2019.
- [10] Xuzhi Lai, Yawu Wang, Min Wu, and Weihua Cao. "Stable Control Strategy for Planar Three-Link Underactuated Mechanical System," *IEEE/ASME Transactions on Mechatronics*, Vol. 21, No. 3, pp. 1345-1356, 2016.
- [11] Xin Gao, Zeyu Ren, Lin Zhai, Qingxuan Jia, and Huihe Liu. "Two-Stage Switching Hybrid Control Method Based on Improved PSO for Planar Three-Link Under-Actuated Manipulator," *IEEE Access*, Vol. 7, pp. 76263-76273, 2019.
- [12] Xu-Zhi Lai, Ya-Wu Wang, Jun-Qing Cao, and Min Wu. "A simple and quick control strategy for a class of first-order nonholonomic manipulator," *Nonlinear Dynamics*, Vol. 85, pp. 2261-2276, 2016.
- [13] Yawu Wang, Xuzhi Lai, Pan Zhang, and Min Wu. "Adaptive robust control for planar n-link underactuated manipulator based on radial basis function neural network and online iterative correction method," *Journal of the Franklin Institute*, Vol. 355, No. 17, pp. 8373-8391, 2018.
- [14] Oussama Khatib. "A Unified Approach for Motion and Force Control of Robot Manipulators: The Operational Space Formulation," *IEEE Journal of Robotics and Automation*, Vol. 3, No. 1, pp. 43-53, 1987.
- [15] Luis Sentis and Oussama Khatib. "Control of Free-Floating Humanoid Robots Through Task Prioritization," *Proceeding of International Conference on Robotics and Automation*, pp. 1718-1723, 2005.
- [16] Marco Hutter, Hannes Sommer, Christian Gehring, Mark Hoepflinger, Michael Bloesch, and Roland Siegwart. "Quadrupedal locomotion using hierarchical operational space control," *The International Journal of Robotics Research*, Vol. 33, No. 8, pp. 1047-1062, 2014.
- [17] Alessandro M. Giordano, Gianluca Garofalo, Marco De Stefano, Christian Ott, and Alin Albu-Schäffer. "Dynamics and control of a free floating space robot in presence of nonzero linear and angular momenta," *Proceeding of IEEE 55th Conference on Decision and Control (CDC)*, pp. 7527-7534, 2016.
- [18] Gianluca Garofalo, Fabian Beck, and Christian Ott. "Task-space tracking control for underactuated aerial manipulators," *Proceeding of 2018 European Control Conference (ECC)*, pp. 628-634, 2018.
- [19] Michael Mistry and Ludovic Righetti. "Operational Space Control of Constrained and Underactuated Systems," *Proceeding of Robotics: Science and System*, p31, 2011.
- [20] Farhad Aghili. "Quadratically Constrained Quadratic-Programming Based Control of Legged Robots Subject to Nonlinear Friction Cone and Switching Constraints," *IEEE/ASME Transactions on Mechatronics*, Vol. 22, No. 6, pp. 2469-2479, 2017.
- [21] Linfeng Li and David J. Braun. "Constrained Feedback Control by Prioritized Multi-objective Optimization," *Proceeding of International Conference on Robotics and Automation*, pp. 9496-9501, 2019.
- [22] David J. Braun, Yuqing Chen, and Linfeng Li. "Operational Space Control Under Actuation Constraints Using Strictly Convex Optimization," *IEEE Transactions on Robotics*, Vol. 36, No. 1, pp. 302-309, 2019.
- [23] Farhad Aghili. "A Unified Approach for Inverse and Direct Dynamics of Constrained Multibody Systems Based on Linear Projection Operator: Applications to Control and Simulation," *IEEE Transactions on Robotics*, Vol. 21, No. 5, pp. 834-849, 2005.
- [24] Michael Mistry, Jonas Buchli, and Stefan Schaal. "Inverse Dynamics Control of Floating Base Systems Using Orthogonal Decomposition," *Proceeding of International Conference on Robotics and Automation*, pp. 3406-3412, 2010.
- [25] Bruno Siciliano, Lorenzo Sciavicco, Luigi Villani, and Giuseppe Oriolo. "Robotics: Modelling, Planning and Control," *Springer Publishing Company*, 2008.
- [26] Farhad Aghili. "Non-Minimal Order Model of Mechanical Systems With Redundant Constraints for Simulations and Controls," *IEEE Transactions on Automatic Control*, Vol. 61, No. 5, pp. 1350-1355, 2016.
- [27] Farhad Aghili. "Inverse and Direct Dynamics of Constrained Multi-body Systems Based on Orthogonal Decomposition of Generalized Force," *Proceeding of International Conference on Robotics and Automation*, pp. 4035-4041, 2003.
- [28] Farhad Aghili and Chun-Yi Su. "Control of Constrained Robots Subject to Unilateral Contacts and Friction Cone Constraints," *Proceeding of International Conference on Robotics and Automation*, pp. 2347-2352, 2016.
- [29] Davide Calzolari, Roberto Lampariello, Alessandro M. Giordano. "Singularity Maps of Space Robots and their Application to Gradient-based Trajectory Planning," *Proceeding of 2020 Robotics Science and Systems (RSS)*, Virtual Conference. 10.15607/RSS.2020.XVI.015, 2020.
- [30] Alessandro M. Giordano, Gianluca Garofalo, and Alin Albu-Schäffer. "Momentum dumping for space robots," *Proceeding of IEEE 56th Conference on Decision and Control (CDC)*, pp. 5243-5248, 2017.